

Structure's base design for earthquake protection numerical and experimental study

K. Alsaif†

King Saud University, Riyadh, Saudi Arabia

H. Kaplan†

Department of Mechanical Engineering, University of Wisconsin-Madison, WI 53706, USA

(Received February 26, 2001, Revised September 6, 2002, Accepted February 6, 2003)

Abstract. A base isolation system is proposed for earthquake protection of structures. The system incorporates spherical supports for the base, a specially designed spring-cam system to keep the base rigidly supported under normal condition and to allow it to move for the duration of the earthquake under the constraint of a spring with optimized non-linear characteristics. A single-story model is constructed to investigate the feasibility of the concept. Numerical simulations of the system as well as experimental results show that 95% reduction of the transmitted force to the structure can be achieved. To demonstrate the effectiveness of this isolation mechanism, the maximum dynamic bending stress developed at pre-determined critical points within the frame of the structure is measured. Significant reduction of the dynamic stresses is obtained.

Key words: earthquake protection; active isolation; transmitted force; dynamic stresses; spherical support.

1. Introduction

Structures with a base isolation system are less vulnerable to damages caused by earthquake disturbances. The current study investigates the feasibility of developing a semi-active system for the protection of structures against earthquakes. The use of active systems for the protection of structures subjected to earthquakes has been the subject of numerous investigations in recent years. Some of the considered design approaches for dealing with this important problem can be found in Kaplan and Seireg (1999).

The effectiveness of active bottom or top vibration absorbers was investigated by Palazzo and Petti (1994) and the tuned column damper was studied by Kareem (1994). Wang and Liu (1994) simulated a hybrid control system for flat-surface base isolation systems with Coloumb friction. The active friction-control of sliding-base isolation systems was studied by Wang and Reinhorn (1989). Because of the low frictional interfaces, an additional mechanism was suggested to control the relative motion of the base to the ground. Jahilal and Utku (1996) investigated the use of an active

† Doctor

control mechanism on passively isolated building by using actuators. Their proposed system can minimize torsional displacements as well as horizontal movements. Systems with Pure-Friction base isolation and Laminated-Rubber Bearing base isolation system have been subject to a good deal of research. Mostaghel and Davis (1997) investigated Coloumb friction effects for a sliding base. They assumed a rigid structure supported on the base isolation system that incorporates a restoring force, a viscous damping force and a friction force. A Coloumb frictional pendulum used as a passive base isolation system for vertical and horizontal effects was analyzed by Almazan and La Llera (1998). They suggested a system which consists of a spherical stainless steel surface and a lentil-shaped articulated slider covered by a teflon-based bearing capacity composite materials. A computational model for the base isolated structures by a ball system with rolling friction on concave surfaces has also been studied by Zhou and Lu (1998).

The system investigated in this study considers a base supported on spherical rollers and equipped with cam devices to restrict the lateral motion of the base and provide a rigid support under normal conditions. The cams are released when an earthquake signal is detected to allow the base to move on the balls for a predetermined period before it comes in contact with springs located around the base. The cams are reactivated after shock wave ends to fully compress the springs and restore the base to its original position. The process is repeated if an after shock is identified by the controlling computer. The geometric design of the base is such that it minimizes any rotational effects due to mass distribution of the structure. A structure model is designed to perform dynamic measurements to verify the numerical simulation of the system. In the tests, two main parameters are considered in the measurements; namely, the transmitted acceleration to the structure and the maximum dynamic stress developed in the frame of the structure.

2. System model

A schematic representation of the systems is given in Fig. 1. The structure is represented by a mass M_s and a spring K_s representing the lateral compliance of the structure. For a multi-degree of freedom structure, M_s would represent the modal mass for the fundamental mode and $K_s = M_s w_n^2$ where w_n fundamental natural frequency of the system. The geometric center of the base is designed to fall directly under the center of the mass of the structure in order to minimize any torsional loads on the base. Each ball is placed between concave surfaces that automatically tend to restore the balls and the base to their original position even if the system undergoes some rotational response.

The force-displacement characteristics for the spring used to limit the movement of the base is illustrated in Fig. 2; where it can be seen that it becomes active after the base is displaced a distance b relative to the ground. The stiffness value K_b represents the equivalent restoring force on the base as it contacts the springs that are placed radially as shown in Fig. 1. In Fig. 3, the spring function K_b is not sensitive to the travel direction of the shock wave for this type of spring arrangement. In this case

$K_b = \sum_{i=1}^5 K(l_i)^2$. Where K is the stiffness of the individual springs and l is the directional cosine for

each spring relative the direction of the displacement.

Accordingly $K_b = 2K$ for the considered case. A diagrammatic representation of the spring cam system used to achieve the desired restoring force characteristics is given in Fig. 4(a).

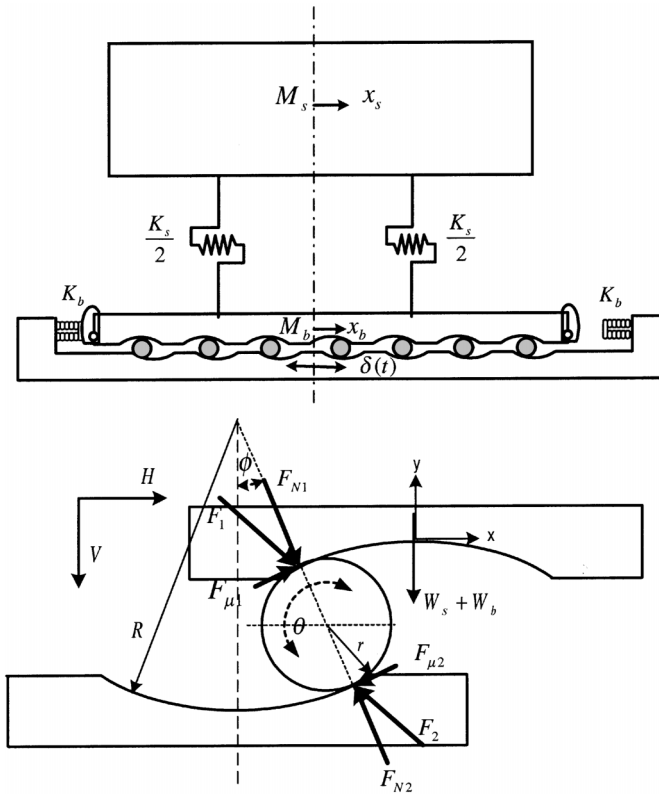


Fig. 1 Motion of the base on the balls with the concave support

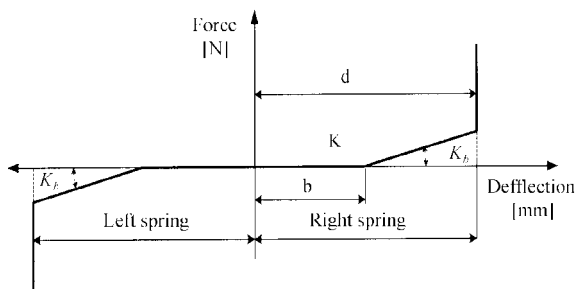


Fig. 2 The force displacement characteristics of the spring

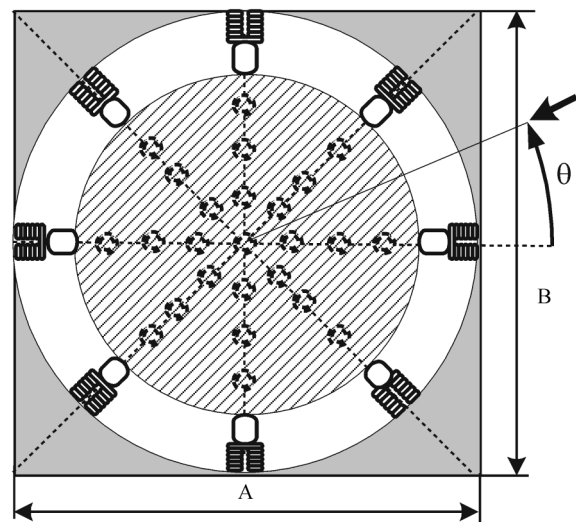


Fig. 3 Top view of the isolated base

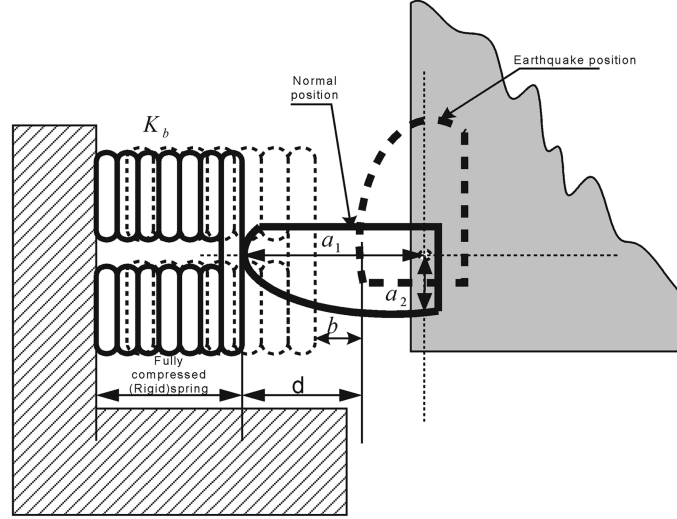


Fig. 4 (a) Diagrammatic representation of the spring cam system

3. Equations of motion

Assuming pure rolling of the balls on the concave surface and neglecting the mass of the balls compared to the structure, the governing equations of motion can be expressed as (for details refer to the appendix):

(a) When the base movement is unconstrained by the spring ($t < t_0$)

$$M_b \ddot{x}_b + K_s(x_b - x_s) + \text{sgn}(\dot{x}_b - \dot{\delta}(t)) \mu_{eff} ((M_s + M_b)(\ddot{y}_b + g)) = 0 \quad (1)$$

$$M_s \ddot{x}_s + K_s(x_s - x_b) = 0 \quad (2)$$

Where

$$\ddot{y}_b = 2(R - r) \left[\left(\frac{\ddot{x}_b - \ddot{\delta}(t)}{R} \right) \sin \left(\frac{(x_b - \delta(t))}{R} \right) + \left(\frac{(\dot{x}_b - \dot{\delta}(t))}{R} \right)^2 \cos \left(\frac{(x_b - \delta(t))}{R} \right) \right] \quad (3)$$

the effective coefficient of friction
$$\mu_{eff} = \left[\frac{(\mu_0 \cos \phi + \sin \phi)}{(\mu_0 \sin \phi - \cos \phi)} \right] \quad (4)$$

the total horizontal force on the base:

$$H = \frac{(\mu_0 \cos \phi + \sin \phi)}{(\mu_0 \sin \phi - \cos \phi)} (M_s + M_b)(g + \ddot{y}_b) \quad (5)$$

the total vertical force on the base:

$$V = (M_s + M_b)(g + \ddot{y}_b) \quad (6)$$

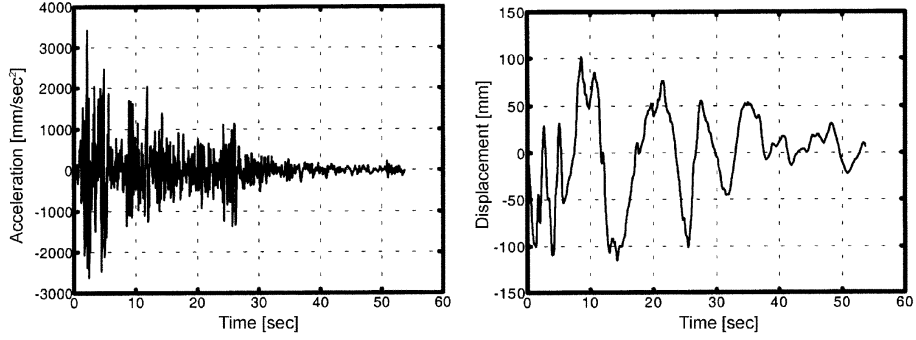


Fig. 4 (b) El-Centro earthquake (S00E component)

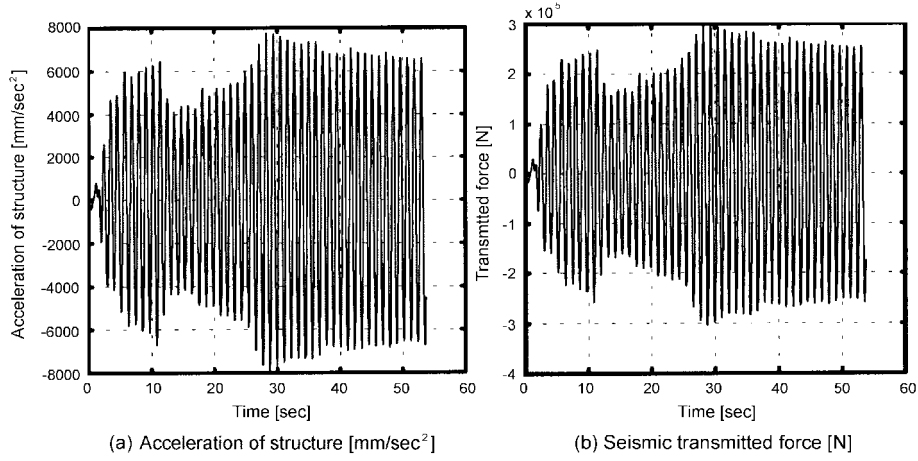


Fig. 4 (c) Response of the rigidly supported structure to the earthquake signal (Case-0)

(b) When the base contacts the foundation springs ($t > t_0$)

$$M_b \ddot{x}_b + K_s(x_b - x_s) + K_b(x_b - \delta(t)) + \text{sgn}(\dot{x}_b - \dot{\delta}(t))\mu_{eff}((M_s + M_b)(\ddot{y}_b + g)) = 0 \quad (7)$$

$$M_s \ddot{x}_s + K_s(x_s - x_b) = 0 \quad (8)$$

4. Numerical simulation results

The non-linear equations of motion are integrated using the 4th order Runge-Kutta numerical scheme. The earthquake signal considered for illustration is that of El-Centro earthquake (S00E) shown in Fig. 4(b).

Case Illustration

The following cases demonstrate the effect of the isolation mechanism on the system response.

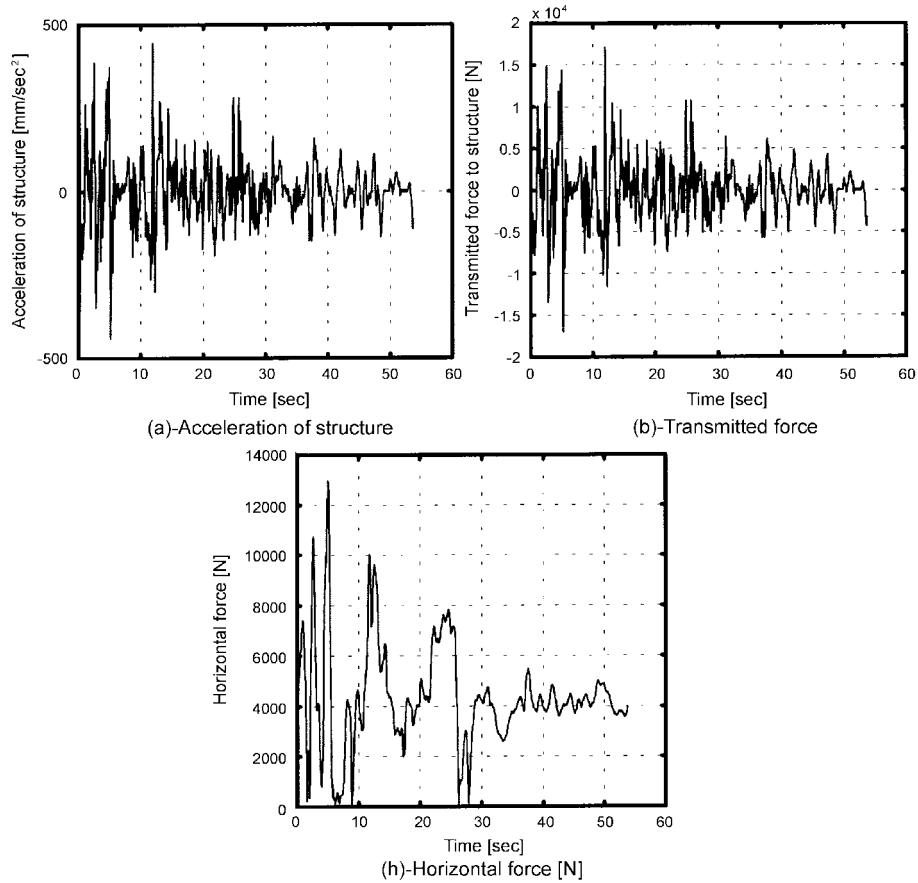


Fig. 5 Response of the system for unconstrained base motion (Case-1)

Non-isolated base:

Case-(0) Rigidly supported base

The results in this case with $M_s = 38500$ Kg, $w_n = 5.88$ r/sec and $\delta = x_b$ are depicted in Fig. 4(c).

Base-isolated:

Case-(1) Unconstrained base motion ($|x_b - \delta(t)| < b$)

For $M_b = 0.05 M_s$ and $\mu_0 = 0.01$ the results are given in Fig. 5.

Balls are used in this case with radius $r = 600$ mm. The radius of the concave support surface is $R = 7r$.

Case-(2) Continuous spring constraint (the base contacts the spring K_b for the duration of the ground wave)

The results for this case with $K_b = 0.05 K_s$ are shown in Fig. 6.

Case-(3) Spring constraints after 5 sec of unconstrained movement

The system in this case is the same as the previous case with the exception that the cams allow

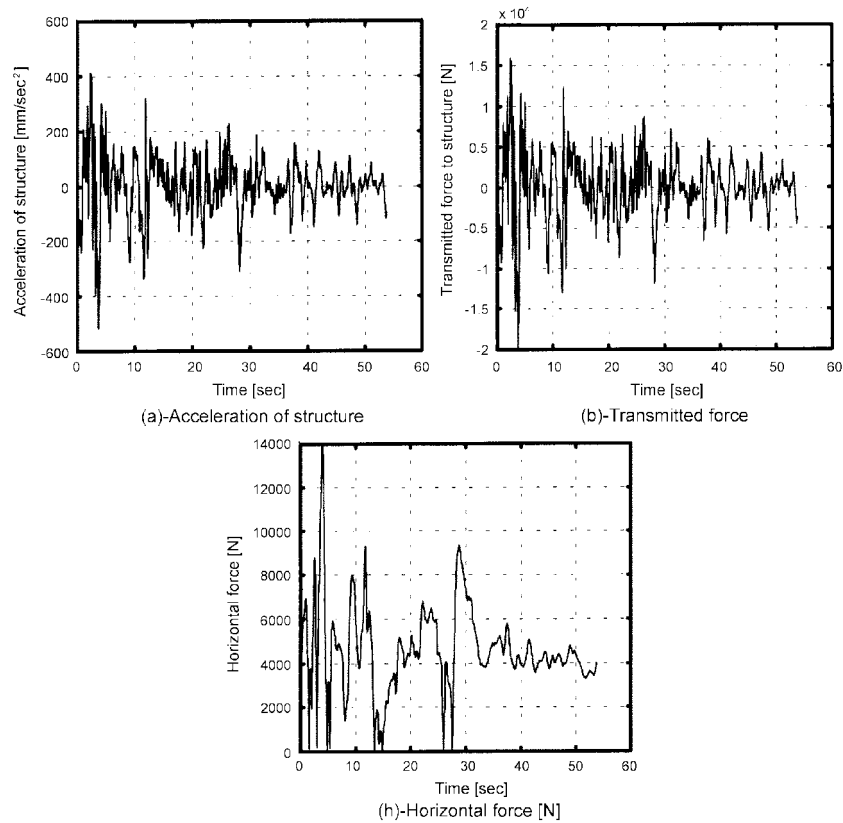


Fig. 6 Response of system with springs in continuously contact with the base for the duration of the shock wave (Case-2) $K_b = 0.05K_s$

the base to move unconstrained for $t_o = 5$ sec after which they are controlled to provide continuous contact with all the springs. The results in this case are given in Fig. 7.

Table 1 shows a summary of the results for the above cases for comparison. It can be seen from Table 1 that case 3 is the best practical design since the transmitted force in this case is reduced about 20 times as opposed to the rigid base support. It should be noted also that the vertical transmitted forces resulting from the spherical support of the balls are negligible in comparison to the weight of the structure.

Table 1 Summary of the numerical results

Case No	Description	Fig. No	Max Trans. Force [N]	Reduction Ratio = $\frac{F_0}{F_{case}}$ [times]
0	Rigid base support	4-c	298,460.0	1
1	Unconstrained base on the balls	5	17,125.0	17.4
2	Spring constrained base on the balls	6	19,922.0	15.0
3	Base spring constrained after 5 sec	7	14,911.0	20.0

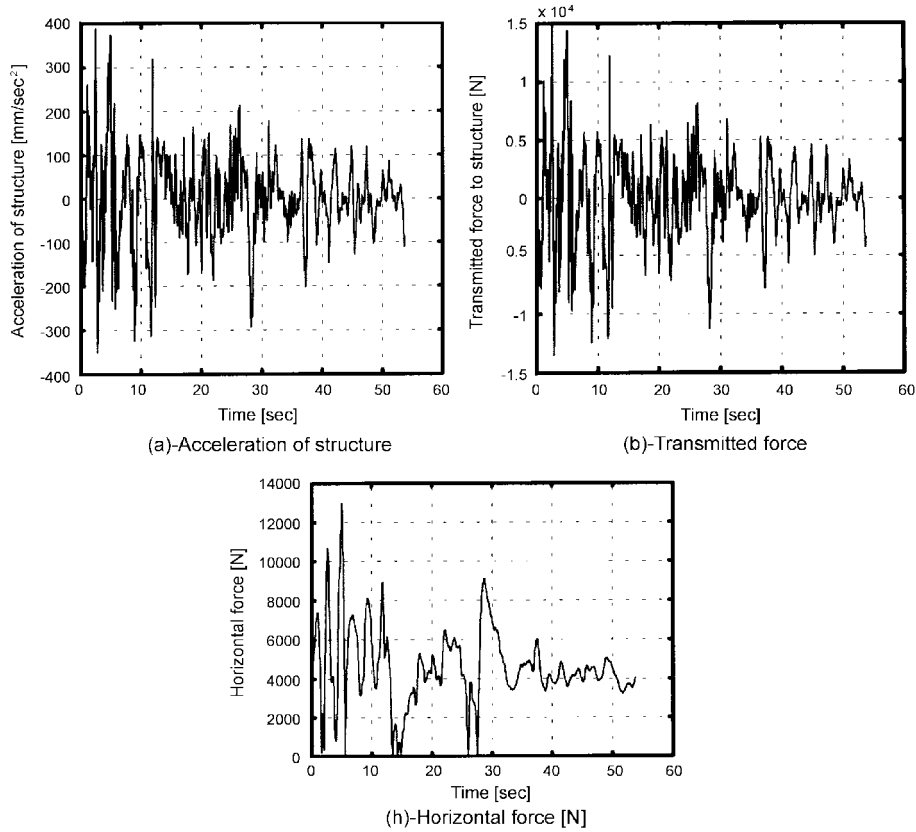


Fig. 7 Response of the system with spring constraint at the base after $t_0 = 5$ sec (Case-3)

5. Qualitative description of the control mechanism

The numerical results for the case (3) treated in the last section suggest that a relatively simple and robust semi-active control can be implemented to protect the structure. Sensors can be placed at a sufficient distance from the structure to allow time for the controller to release the positioning cams. Once the signal is detected, the movement of the cam can be controlled based on pre-programmed information of the earthquake function to allow unconstrained motion of the base that is best suited for the disturbance function. The cams can be rotated to keep the base in contact with the spring after a time t_o from the onset of its motion. When the shock wave departs, the control system would allow the actuators to rotate the cams in order to restore the base to its original position with the springs fully compressed. The controlling computer is then reset for the next event whenever it occurs.

6. Experimental verification

In this section, few tests are designed and carried out to evaluate the performance of the proposed isolated system.

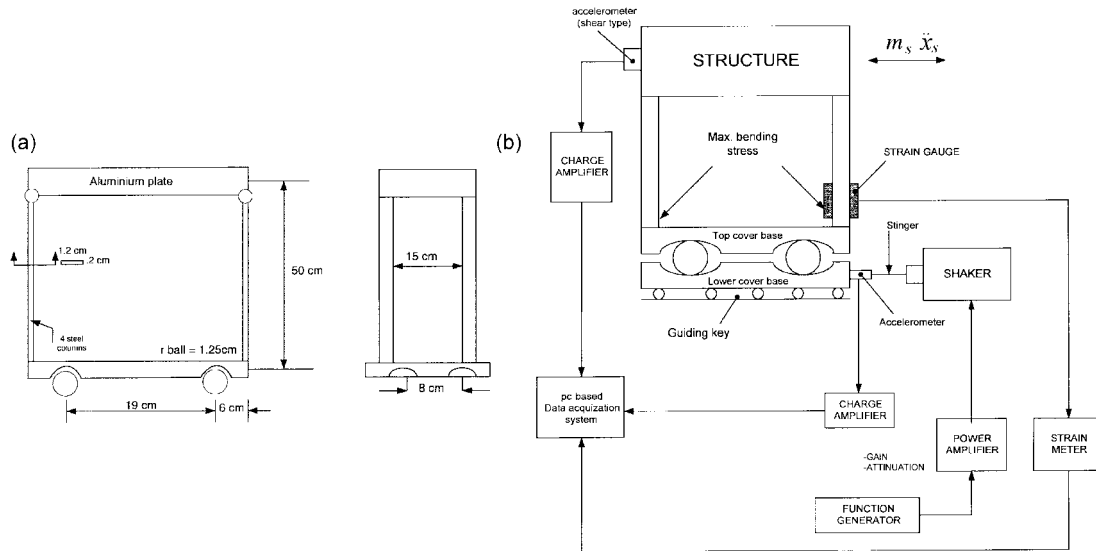


Fig. 8 (a) Single story model dimensions, (b) Experimental set-up (Isolated single-story structure)

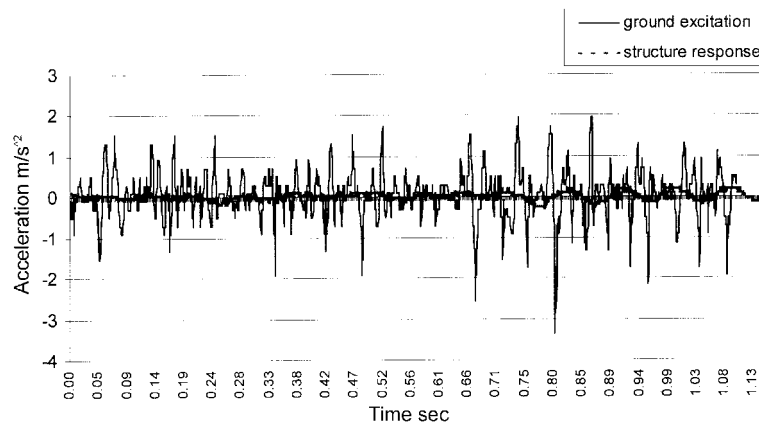


Fig. 9 Time history of the input and output accelerations - Isolated base

6.1 Transmitted acceleration measurements

The transmitted acceleration to the structure, due to imparting a random ground excitation at the base of the model, is measured using shear type accelerometers. Fig. 8 shows the model configuration and the experimental set-up. The single-story building consists of 4 columns, made of steel, to support the first floor. An electrodynamic shaker provides the input acceleration. The strength of the input excitations can be changed by increasing/decreasing the gain of the power amplifier. The signal from the accelerometer is conditioned using a charge amplifier and connected to a data acquisition system. It should be mentioned that the base of the structure is allowed to move freely during the input ground excitation. A sample result of the time history of the input excitation and the output response of the structure for the base-isolated system is shown in Fig. 9. It can be

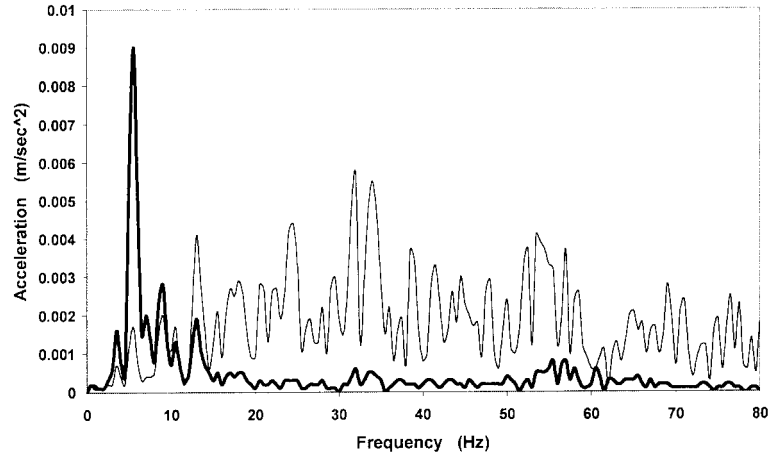


Fig. 10 The frequency spectrum of the input acceleration (thin line) and the output acceleration (bold line)- (non-isolated base)

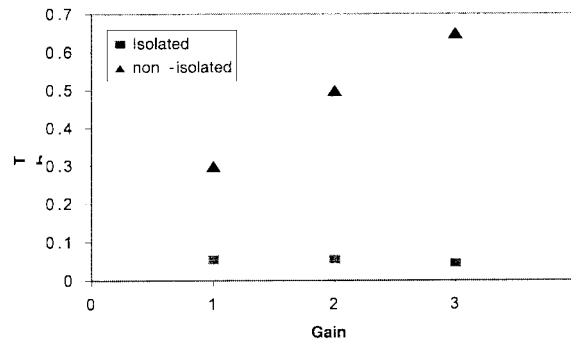


Fig. 11 The transmissibility ratio of the isolated structure-base system with different input gains

seen that a very high attenuation in the transmitted acceleration is achieved. Fig. 10 shows the frequency spectrum for the case of non-isolated base. The figure shows a distinct peak at about 6 Hz. This frequency component represents the fundamental mode of the structure. A high acceleration amplitude is clearly shown in comparison with the input excitation. It can also be noticed that the contribution of the high frequency components associated with the input excitation is negligible.

The acceleration transmissibility ratio (T.R.), defined as the transmitted acceleration divided by the input acceleration, is obtained for the three different input gains.

Fig. 11 shows the T.R. versus the input gain for both isolated and non-isolated base system (i.e., the balls are removed and the base is rigidly connected to the ground). It can be seen that the transmitted acceleration and hence the transmitted force can be reduced approximately 20 times of the ground excitation or 95% reduction ratio.

For the case of a rigid base, the transmitted acceleration to the structure reached up to 65% of the ground acceleration as shown in the Figure. Obviously, in this case, the 35% reduction of the input acceleration comes from the low bending stiffness of the columns.

6.2 Dynamic strain measurement

The dynamic strain is measured using the experimental setup depicted in Fig. 8. The dynamic bending stress is expected to be maximum at the bottom of each column as shown in the figure. In this case the base of the structure is subjected to a horizontal random ground excitations with three different input gains (g_1 , g_2 and g_3). The maximum stress developed in the columns is measured using electrical strain gages. The electrical signal produced by the strain gages is fed to a conditioning circuit with a programmable amplifier. The analog signal is then converted to digital form using a 12-bit A/D converter. The digital signal is then analyzed to obtain the dynamic strain time history. The corresponding stress signal, S_y , can be obtained from Hook's law. This stress is normalized by a factor S_o defined as;

$$S_o = \frac{F_0}{A} = \frac{m_s \cdot (a_{input})_{r.m.s}}{t \cdot b}$$

Where, $(a_{input})_{r.m.s}$ is the root-mean square of the input acceleration, t is the column thickness and b its width.

The tests are carried out for both cases; isolated and non-isolated structure. A portion of the time history of the input excitations with gain g_3 is shown in Fig. 12. The corresponding dynamic stress normalized to S_o , for the isolated base, is depicted in Fig. 13. Fig. 14 shows the time history of the maximum dynamic stress for the non-isolated structure under the same input excitation (gain = g_3) shown in Fig. 12. One can observe that the maximum dynamic stress ratio S/S_o , within the given range of time, is about 900. This magnitude is about 6 times larger than the corresponding maximum value obtained from Fig. 13 for the base-isolated case. This significant reduction in the bending stresses would consequently reduce the chances of column failure and would improve the safety of the structure. In summary, the dynamic bending stress in the building columns is significantly minimized by using the proposed isolation mechanism.

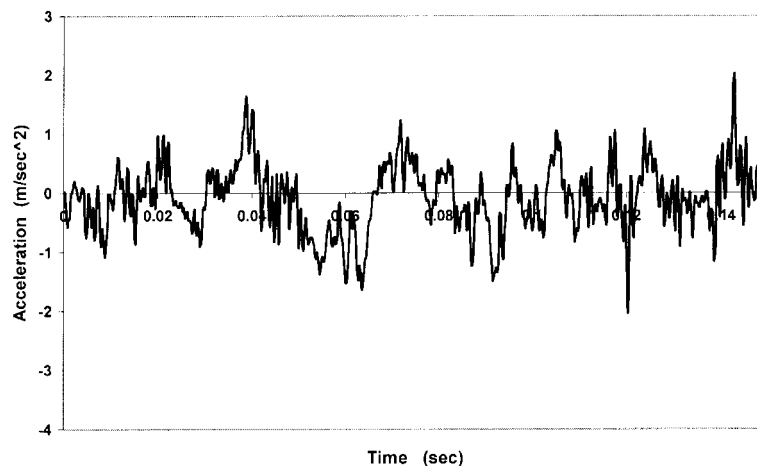


Fig. 12 Portion of the time history for the ground excitation, gain 3

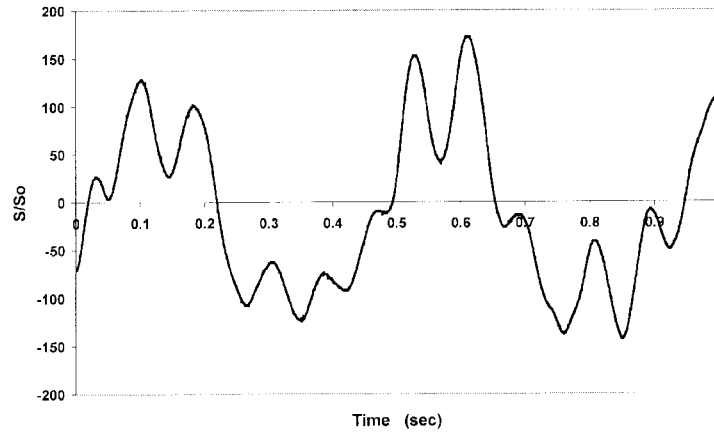


Fig. 13 Maximum dynamic stress vs. time for ground input, gain 3 (isolated base)

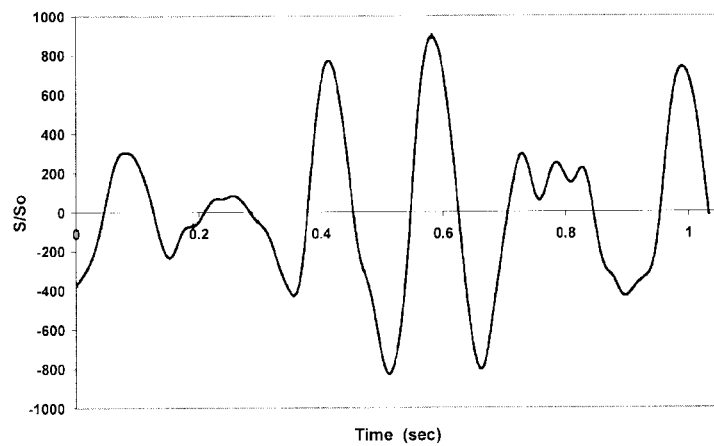


Fig. 14 Maximum dynamic stress vs. time, input gain 3 (non-isolated base)

7. Conclusions

The investigation reported in this paper suggests that a considerable protection of structures subjected to earthquakes can be achieved by the appropriate design of a semi-actively controlled base. Computer controlled cams are used to provide rigid support under normal conditions, to free the base to move on specially designed ball supports for a predetermined period and to keep the base in contact with the foundation spring afterwards for the remainder of the disturbance. Experimental results show that 95% reduction of the transmitted acceleration to the structure can be achieved. Furthermore, the illustrative example of the single-story structure shows that the maximum bending stress generated at pre-determined critical points in the structure columns is significantly reduced. The computer simulation of the case illustration shows that a 20 times reduction of the transmitted force can be attained as opposed to the rigidly supported base and that the system can be readily repositioned for protection against future shocks.

References

- Almazan, J.L. and De La Llera, J.D. (1998), "Modelling aspects of structures isolated with the frictional pendulum system", *Earthq. Eng. Struct. Dyn.*, **27**, 845-867.
- Jahilal, P. and Utku, S. (1996), "Active control in passively base isolated buildings subjected to lower power excitations", *Comput. Struct.*, **66**(2-3), 423-440.
- Kaplan, K. and Seireg, A. (1999), "A computer controlled system for earthquake protection of structures", *Int. J. Computer Applications in Technology*, **13**(1/2).
- Kareem, A. (1994), "The next generation of tuned liquid dampers", *First World Conf. on Structure Control*, Los Angeles, California, USA.
- Mostaghel, N. and Davis, T. (1997), "Representations of Coloumb friction for dynamic analysis", *Earthq. Eng. Struct. Dyn.*, **26**, 541-548.
- Palazzo, B. and Petti, L. (1994), "Seismic response control in base isolation systems using tuned mass dampers", *First World Conf. on Structure Control*, Los Angeles, California, USA.
- Wang, Y.P. and Liu, C.J. (1994), "Active control of sliding structures under strong earthquakes", *First World Conf. on Structural Control*, Los Angeles, California, USA.
- Wang, Y.P. and Reinhorn, A.M. (1989), "Motion control of sliding isolated structures", *Seismic, Shock and Vibration Isolation*, edited by Chung, H. and Fujita, T., **181**, ASME.
- Zhou, Q. and Lu, X. (1998), "Dynamic analysis on structures base isolated by a ball system with restoring property", *Earthq. Eng. Struct. Dyn.*, **27**, 773-791.

Appendix

Geometric relationships and effective coefficient of rolling friction for concave support

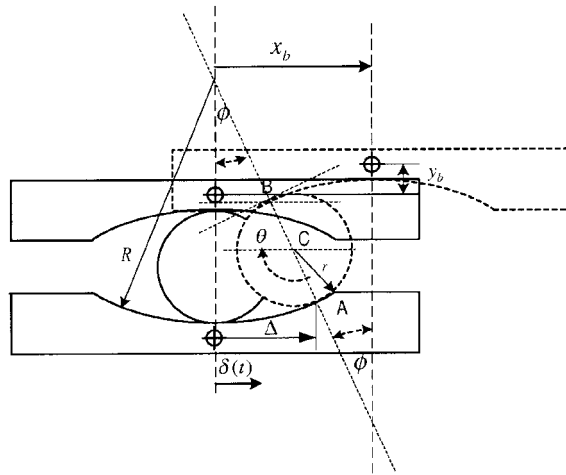


Fig. (a) Motion of the base and geometric relationships; x_b : Displacement of the base, $\delta(t)$: Displacement of the ground

Total horizontal force at the base (n : # of balls)

$$H = (nF_{\mu 1} \cos \phi + nF_{N1} \sin \phi)$$

Total vertical force at the base

$$V = (nF_{N1} \cos \phi - nF_{\mu 1} \sin \phi)$$

The effective coefficient of friction is defined as;

$$\mu_{eff} = \frac{H}{V} = \frac{(nF_{\mu 1} \cos \phi + nF_{N1} \sin \phi)}{(nF_{N1} \cos \phi - nF_{\mu 1} \sin \phi)}$$

$$F_{\mu 1} = \mu_0 F_{N1} \quad (\text{note, } \mu_0: \text{Rolling friction coefficient})$$

$$\mu_{eff} = \frac{H}{V} = \frac{(\sin \phi + \mu_0 \cos \phi)}{(\cos \phi - \mu_0 \sin \phi)}$$

$$\mu_{eff} = \left[\frac{\sin \left[\frac{(x_b - \delta(t))}{R} \right] + \mu_0 \cos \left[\frac{(x_b - \delta(t))}{R} \right]}{\cos \left[\frac{(x_b - \delta(t))}{R} \right] - \mu_0 \sin \left[\frac{(x_b - \delta(t))}{R} \right]} \right]$$

Dynamic equations of the base

$$\sum F_x = M_b \ddot{x}_b$$

$$x_b = \delta(t) + 2(R-r) \sin \phi$$

$$\dot{x}_b = \dot{\delta}(t) + (R-r) [\dot{\phi} \cos \phi]$$

$$\ddot{x}_b = \ddot{\delta}(t) + (R-r) [\ddot{\phi} \cos \phi - \dot{\phi}^2 \sin \phi]$$

For $|x_b - \delta(t)| \geq b$

$$M_b \ddot{x}_b + K_s(x_b - x_s) + K_b(x_b - \delta(t)) \mp (nF_{\mu 1} \cos \phi + nF_{N1} \sin \phi) = 0$$

For $|x_b - \delta(t)| < b$, there is no contact with K_b . The equation of motion can be written as

$$M_b \ddot{x}_b + K_s(x_b - x_s) \mp (nF_{\mu 1} \cos \phi + nF_{N1} \sin \phi) = 0$$

$$M_b \ddot{x}_b + K_s(x_b - x_s) + K_b(x_b - \delta(t)) \mp nF_{N1}(\mu \cos \phi - \sin \phi) = 0$$

$$M_b \ddot{x}_b + K_s(x_b - x_s) + K_b(x_b - \delta(t)) + \text{sgn}(\dot{x}_b - \dot{\delta}(t)) \left| \frac{(\mu_0 \cos \phi + \sin \phi)}{(\mu_0 \sin \phi - \cos \phi)} \right| ((M_s + M_b)(\ddot{y}_b + g)) = 0$$

$$M_b \ddot{x}_b + K_s(x_b - x_s) + K_b(x_b - \delta(t)) + \text{sgn}(\dot{x}_b - \dot{\delta}(t)) \mu_{eff} ((M_s + M_b)(\ddot{y}_b + g)) = 0$$